ISSN 1075-7015, Geology of Ore Deposits, 2006, Vol. 48, No. 4, pp. 304–325. © Pleiades Publishing, Inc., 2006.
Original Russian Text © G.V. Novikov, I.V. Vikent'ev, O.Yu. Bogdanova, 2006, published in Geologiya Rudnykh Mestorozhdenii, 2006, Vol. 48, No. 4, pp. 351–374.

Sorption of Heavy Metal Cations by Low-Temperature Deposits of Pacific Hydrothermal Fields

G. V. Novikov[a], I. V. Vikent'ev[b]*, and O. Yu. Bogdanova[a]

[a] *Shirshov Institute of Oceanology, Russian Academy of Sciences, Nakhimovskii pr. 36, Moscow, 117997 Russia*
[b] *Institute of Geology of Ore Deposits, Petrography, Mineralogy, and Geochemistry, Russian Academy of Sciences, Staromonetnyi per. 35, Moscow, 119017 Russia*

Received May 15, 2005

Abstract—Cation exchange reactions with participation of heavy metals Mn, Co, Ni, Cu, Zn, Cd, Ba, and Pb were studied in oceanic low-temperature hydrothermal deposits of various mineral compositions and in hydrogenic Fe–Mn crusts. Individual minerals and their assemblages differ significantly in absorptive capacity, which increases in the following order: hematite ⩽ Si-protoferrihydrite < protoferrihydrite < goethite < nontronite ⩽ Fe-vernadite + Mn-feroxyhyte < Fe-free vernadite < bernessite + Fe-free vernadite < bernessite; i.e., it successively increases from the mineral with a coordination type of lattice to minerals with a layer-type structure. The exchange complex of all minerals includes Na^+, K^+, Ca^{2+}, and Mg^{2+}, i.e., the main cations of seawater. In Mn minerals, Mn^{2+} is the main exchange component. The contribution of all the mentioned cations to the exchange capacity of minerals is as high as 90–98%. The highest absorptive capacity among the examined low-temperature oceanic deposits is characteristic of hydrothermal Mn minerals. Their capacity exceeds substantially that of hydrothermal oxides, hydroxides, Fe-aluminosilicates, and hydrogenic Fe–Mn minerals. The absorptive capacity of all examined Mn minerals relative to heavy metals increases in the same order: Ni < Zn < Cd < Mn < Co < Pb < Cu.

DOI: 10.1134/S1075701506040052

INTRODUCTION

Low-temperature sorption may be considered a mechanism responsible for the formation of anomalous metal concentrations in the process of lithogenesis because many ore-forming elements are efficiently extracted from natural waters and accumulate in sediments (Chelishchev et al., 1992; Angove et al., 1998; Lead et al., 1999; Takahashi et al., 1999). During epigenetic hydrothermal processes associated with pulses of magmatic or tectonic activity, metallogenically specialized sedimentary sequences could serve as a source of mobilized metals, in addition to their supply from deep-seated chambers. The concept of recycling of primary metal concentrations by subsequent processes (Schneiderhöhn, 1952) remains popular and is used in models of polygenetic deposits (U–Bi–Co–Ni–Ag, Cu, Pb–Zn, etc.). Therefore, the forms of primary syngenetic accumulation of dispersed metals in the course of sedimentation remain an important subject of investigations.

The diversity of viewpoints on mechanisms of syngenetic concentration of metal ions by different minerals can be reduced, in fact, to the following two models: either microcomponents precipitate along with macrocomponents from seawater during the formation of mineral phases or the microcomponents are adsorbed on the surface of earlier phases. It is assumed that precisely sorption controls the microcomponent chemical composition of aluminosilicates, phosphates, and Mn and Fe minerals in almost all oceanic sediments (Strakhov et al., 1968; Volkov, 1979; Cronan, 1980; Andreev, 1994), although experimental data that would confirm this statement are scarce.

Indeed, sorption is one of the main physicochemical processes responsible for differentiation of metal ions during mineral formation in the ocean. The ion exchange properties of many natural compounds such as aluminosilicates, phosphates, carbonates, Mn oxides–hydroxides, and Fe hydroxides provide differentiation of elements owing to interaction between suspended particles of these minerals and seawater and to filtration of the latter through the sedimentary sequence and underlying rocks. In the ocean, sorption proceeds relatively intensely, particularly at the active water–sediment geochemical barrier, owing to the continual contact of mineral phases with surface, bottom, and interstitial seawater.

There are also other reasons why the problem of heavy metal ion sorption has recently attracted the attention of researchers. Interaction at the liquid–solid interface controls migration and stabilization of metal ions in natural low-temperature systems such as sediments of shallow-water reservoirs, drainage networks of ground and human-made facilities, and the oceanic shelf near urbanized areas, i.e., in systems with a highly disturbed ecological equilibrium.

*Address for correspondence: I.V. Vikent'ev. E-mail: viken@igem.ru

The recent metalliferous sediments associated with hydrothermal vents at the oceanic bottom also may be enriched in heavy metals owing to their sorption by particles of Fe and Mn hydroxides (Butuzova, 1998; Schaller et al., 2000), although the mechanisms of this phenomenon remain ambiguous as yet. Of the total diversity of oceanic sediments, only pelagic Fe–Mn nodules and sedimentary crusts from seamounts have been subjected to systematic experimental studies to determine their sorption properties (Chelishchev et al., 1992; Novikov and Yashina, 1993; Novikov et al., 1995; Novikov, 1996; Novikov and Skornyakova, 1998; Novikov and Cherkashev, 2000). It was established that they are highly selective natural sorbents of metal ions, primarily, cations of heavy and rare metals, and are characterized by high exchange capacity, selectivity coefficients, and kinetic parameters. Fe–Mn nodules and crusts can efficiently absorb cations of heavy and rare alkali metals from natural waters, which provides high metal concentrations therein.

At the same time, oceanic low-temperature hydrothermal deposits, largely composed of Mn oxide–hydroxides, Fe hydroxides, aluminosilicates, and sulfates, are interesting objects for study with regard to their ion exchange properties. With respect to their spatial distribution and genesis, these deposits occupy an intermediate position between sulfides deposited near hot hydrothermal vents, on the one hand, and metalliferous sediments that form dispersion halos at flanks of hydrothermal fields distant from discharge zones of relatively high-temperature sulfide-forming fluids, on the other hand (Lisitsyn et al., 1991; Bogdanov et al., 2004).

Using a complex of mineralogical and geochemical methods, we studied low-temperature hydrothermal sediments and hydrogenic Fe–Mn crusts sampled by Pisces manned submersibles in the peripheral zone of the Juan de Fuca hydrothermal field (Axial Seamount) during Cruise 12 of the R/V *Akademik Mstislav Keldysh* in 1986 (Bogdanov et al., 2004) and by a Mir deepwater manned submersible in the active low-temperature field of Franklin Seamount during Cruise 21 of the same research vessel in 1990 (Lisitsyn et al., 1991). At *Axial Seamount*, brick red ochers are developed at the surface of basalt at boundaries between neighboring pillows and in a system of chaotically oriented fissures that appeared in the course of basaltic lava solidification. The ochers consist almost entirely of well-preserved relicts of ferruginous bacteria morphologically identical to *Gallionella* or, less commonly, *Siderocapsa* and *Siderococcus* (Bogdanova and Gorshkov, 1987). The perfect preservation of bacterial relicts during a long period (4 ka) is explained by simultaneous accumulation of Fe hydroxides and silica at the surface of bacteria. Ochers are largely composed of protoferrihydrite and ferrihydrite as a product of protoferrihydrite recrystallization. Some samples contain an admixture of hematite. The black crusts 1.5–2.0 mm thick observed at the surface of basaltic flows at some distance from the hydrothermal field are composed of Fe-free vernadite with less abundant bernessite. Ochers are locally covered by hydrogenic films approximately 1 mm thick that are composed of Fe-vernadite closely associated with Mn-feroxyhyte and goethite.

Hydrothermal deposits of *Franklin Seamount* make up irregularly shaped mounds from a few centimeters to 7 m high. Most of these mounds are characterized by a similar internal structure (Bogdanova et al., 1990; Gorshkov et al., 1992). Their surface is locally coated with Mn crusts from 1 mm to 2 cm thick. The crusts are underlain by bright orange, highly porous matter a few tens of centimeters thick, which gives way down the section to a dark green, finely dispersed substance. Thus, there are three types of sediments regularly replacing each other from the peripheral part of the hydrothermal mound toward its center.

RESEARCH METHODS

Analytical transmission electron microscopy (ATEM) was used in this study. A sample of approximately 50 mg in weight was taken to prepare an aqueous suspension with a UZDN-2T ultrasonic disperser. A drop of suspension diluted to the desirable state was placed on a cathodic film substrate and dried. The study was carried out on a JEM-100C electron microscope under an accelerating voltage of 100 kV. The microscope was equipped with a goniometer that provided an inclination of ±60°. Microdiffraction of electrons was the main method used for identification of mineral phases. Their composition was controlled by a KEVEX-5100 spectrometer.

Exchange reactions between water solutions of metal salts with concentrations C_0 = 1.0–0.001 g-equiv/l and low-temperature hydrothermal and hydrogenic deposits were used for the study of their sorption properties under similar conditions irrespective of the mineral compositions of samples. Experiments were conducted in the static regime at a temperature of 20 ± 1°C and intense stirring of phases with a constant liquid/solid proportion equal to 100. When nontronite and Fe–Mn minerals dominated in samples, the charge was as heavy as 100–150 mg, while the samples consisting of hydrothermal Mn minerals weighed 30–50 mg. For all samples, the sorption of metal cations was studied in three parallel runs with solution concentrations C_0 = 1.0 and 0.001 g-equiv/l (the upper and lower limits in the studied interval of concentrations) and in two parallel runs with concentrations C_0 = 0.1 and 0.01 g-equiv/l. The reproducibility of measurements was 98.1–99.3%. Nitrate (Ni, Co, Cu, Cd, Pb), chloride (Mn), and sulfate (Zn) solutions were used in experiments.

The runs were carried out as follows. The charge was placed into a glass test tube, a metal salt solution was poured over the charge, and the tube was stoppered. Test tubes were inserted into a device allowing

their rotation through 360° to provide a uniform distribution of solid particles throughout the solution.

The period to attain equilibrium cation species of mineral assemblages was 7–10 days, which, according to experimental data (Chelishchev et al., 1992; Novikov and Cherkashev, 2000; Novikov, 2005), was sufficient to establish equilibrium. The pH of solutions was measured before and after the runs with an EV-74 ionometer. After sorption runs, phases were separated on the blue ribbon paper filter. The solid phase was washed with distilled water, dried at room temperature up to a constant weight, and then decomposed in the appropriate reagents. First the pH and then the concentrations of metal ions were determined in equilibrium solutions.

The acid decomposition of aluminosilicate samples was carried out in line with the procedure described by Ponomarev (1963). The samples consisting of Fe minerals were first decomposed in a mixture of concentrated HF + $HClO_4$ solutions. The dry residue was then additionally dissolved in 7% HCl solution, and both solutions were poured into a single retort, where they were diluted with distilled water up to a desirable level. The samples composed of Mn minerals were dissolved in a mixture of concentrated HCl + H_2O_2 solutions by boiling for 3–5 min. The metal cation concentrations in the respective solutions were measured with flame atomic absorption spectroscopy (AAS) on a Perkin–Elmer 503 device at the analytical laboratory of the Institute of Oceanology, Russian Academy of Sciences, by N.N. Zavadskaya, L.A. Fedorova, and N.P. Tolmacheva. The difference between the AAS results and concentrations of elements in standard samples was estimated by the *t*-test (Doerfel, 1969). The differences were insignificant at a confidence level of 0.95.

Particular attention was paid to the samples composed of Mn minerals with possible occurrence of Mn (IV) and (II). Like concentrations of other metals, the Mn (II) content was determined with AAS after its preliminary extraction from a separate charge by 1% H_2SO_4 solution (Bazilevskaya, 1986).

MINERAL ASSEMBLAGES OF LOW-TEMPERATURE DEPOSITS

The deposits of the first type are composed of *Mn minerals*: either of bernessite (sample 2157-14a) or a mineral assemblage of hexagonal, monoclinic, and triclinic bernessite and Fe-free vernadite (samples 1845-10b, 2202-2A1b, and 2202-2B2) (Table 1). Bernessite is represented by platy particles and thin scaly aggregates characterized by the hexagonal unit cell with parameters $a = 2.83$ Å and $c = 7.1$ Å, as well as by minerals described previously as 14-Å bernessite with the orthorhombic unit cell and clinobernessite (Bogdanova and Gorshkov, 1987). Different aggregates of the examined minerals differ in the spatial ordering of their structure. Some scaly aggregates are characterized by a relatively ordered structure, but most of them are poorly ordered, determining the generally disordered structure of the examined bernessites. Platy bernessite microcrystals make up frequent regular intergrowths with one another. Bernessite is often associated with replacing Fe-free vernadite.

The Mn content in low-temperature hydrothermal Mn minerals ranges from approximately 21 to 31 wt %, while the Fe content is lower by no less than an order of magnitude: 0.84–3.02 wt % (Table 1). Among all examined assemblages, Mn minerals are characterized by the lowest Si contents (1.45–10.80 wt %) and are intermediate between nontronite and Fe minerals in Al concentrations (0.33–1.88 wt %). The contents of heavy metals (Cu, Co, Ni, etc.) are low and range from thousandths to tens of thousandths of a percent.

The Mn and Fe contents in hydrogenic Fe–Mn crusts (samples 1479-2a, 1845-10a, 1863-2, etc.; Table 1) are similar and vary from 9 to 20 wt %. In contrast to hydrothermal Mn and Fe minerals, the concentrations of heavy metals in these samples are one to two orders of magnitude higher: from tenths to hundredths of a percent.

In the second mineral assemblage, the main phases are represented by *protoferrihydrite* (samples 1491-1, 1863-4, 2218-6, and 2192-2(2)b) and *Si-bearing protoferrihydrite* (samples 2157-10, 2157-11, 2157-14, and 2170-7) (Fig. 1a) accompanied by subordinate nontronite (samples 2192-2(2)b, 2170-2(2), 2170-4, and 2202-2A1.a) and sporadic hematite (samples 1863-4, 2202-2A2.2, 2202-2A2.3, and 2202-2A2.4). Electron diffraction patterns obtained for Fe hydroxide particles (Fig. 1b) contain two diffuse ring reflections with *d* approximately equal to 2.5 and 1.45 Å, indicating only two-dimensional ordering of this hydroxide, i.e., extremely small sizes of coherent dispersion areas. Fe hydroxide particles contain silica and are mineralized relicts of pedicellate bacteria belonging to the genus *Gallionella.* Si-bearing protoferrihydrite contains phosphorus (frequently up to 4–5 wt %), which indicates a sufficiently young age of the hydrothermal mound, and rare ferrihydrite particles (sample 2202-2A1.a) as products of recrystallization of protoferrihydrite during aging of its individual particles.

Nontronite in these samples occurs as scaly aggregates (Figs. 1c, 1d). The microdiffraction study of nontronite demonstrates that the mineral is characterized by a highly disordered structure: relatively slight basic *hk* and basal (*001*) reflections were recorded. Nontronite scales are closely associated with Si-bearing protoferrihydrite.

The Fe content in Fe minerals, Si-bearing protoferrihydrite included, ranges from 12.85 to 50.00 wt % (Table 1). There is no notable difference in this parameter between samples composed practically of a single phase (hematite, goethite, or protoferrihydrite) and samples consisting of several mineral phases. The Mn content in Fe minerals varies from 0.052 (hematite) to 2.64 wt % (protoferrihydrite). Sample 2202-2A2.2,

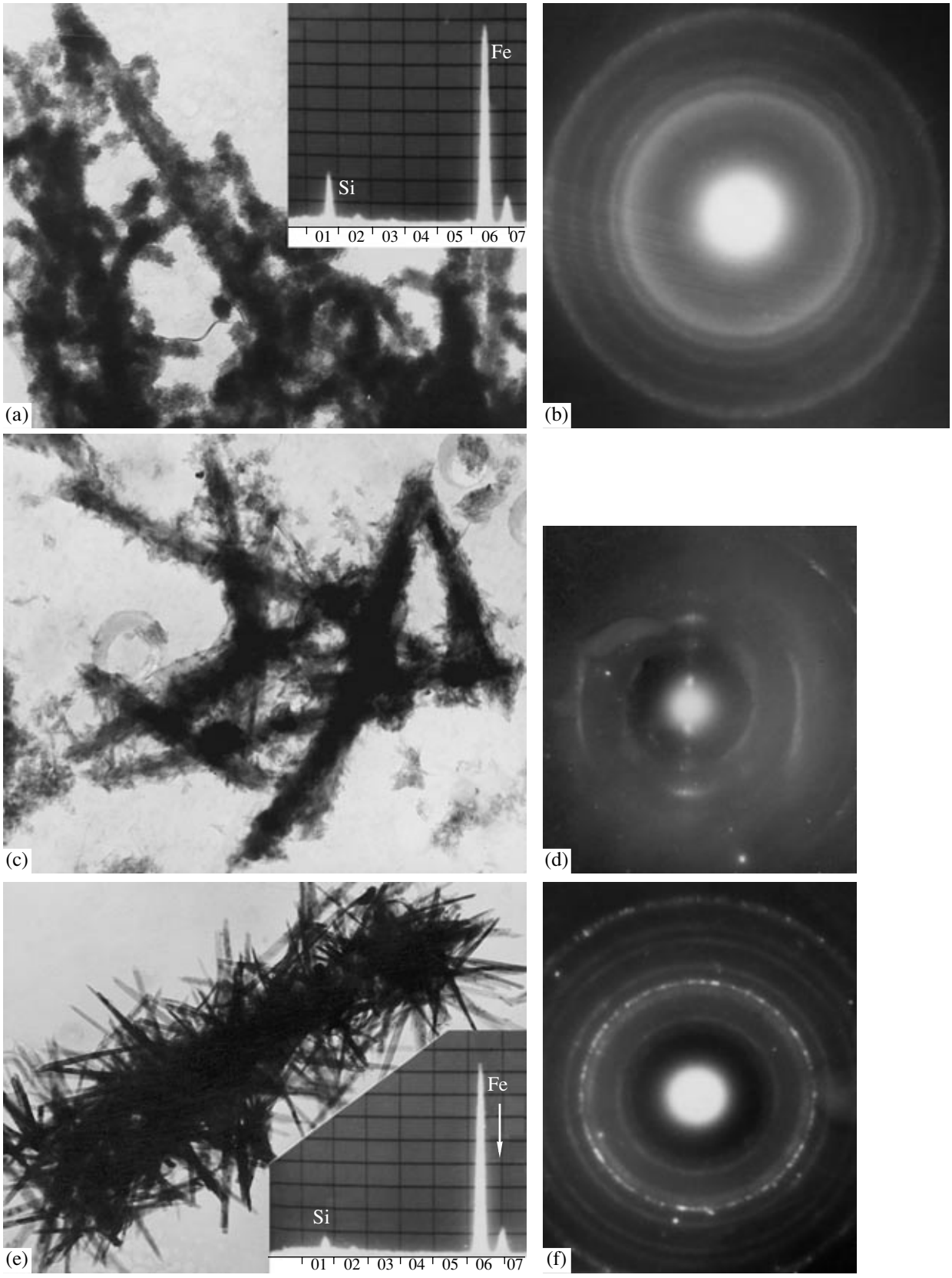

Fig. 1. (a, c, e) SEM images and energy dispersive spectra and (b, d, f) electron diffraction patterns of mineral aggregates from low-temperature deposits. (a, b) Bacteria-like particles of Si-bearing protoferrihydrite, magn. 55000; (c, d) nontronite, magn. 75000; and (e, f) hematite, magn. 40000.

Table 1. Chemical and mineral compositions of Fe and Mn deposits from Pacific hydrothermal fields

Type of hydrothermal deposits	Sample number	Mineral composition	Content of components													
			Si	Al	Fe	Mn_{tot}	Ni	Co	Cu	Zn	Pb	Ba	Ca	Mg	Na	K
			wt %				10^{-4} wt %					wt %				
1	2	3	4	5	6	7	8	9	10	11	12	13	14	15	16	17
Franklin Seamount																
Small hydrothermal mounds composed of Fe hydroxides	2157-6	Nontronite	19.76	0.26	40.75	0.26	54	37	140	164	24	0.082	2.76	1.86	5.64	0.42
	2157-7	Nontronite and protoferrihydrite (small amounts)	21.85	0.32	47.14	0.88	1.52	83	94	72	65	0.066	2.18	1.36	2.76	0.58
	2157-10	Si-bearing protoferrihydrite with high (up to 4%) P content	15.20	2.26	43.25	2.24	15	72	13	10	15	0.036	1.04	1.25	4.66	0.71
	2157-11	Si-bearing protoferrihydrite with high (up to 5%) P content	16.74	2.64	31.36	1.30	96	9	60	110	32	0.184	8.69	2.10	8.27	0.67
	2157-14	Si-bearing protoferrihydrite	17.44	3.03	33.90	1.26	64	73	113	108	13	0.034	0.83	0.94	7.42	0.64
Black film on loose ocherous ferruginous material	2157-14a	Hexagonal, monoclinic, and triclinic bernessite	1.45	0.33	2.46	30.84	956	307	343	288	62	0.43	2.40	1.84	2.06	0.72
Small hydrothermal mound:	2170-2(1)	Fe-vernadite and Mn-feroxyhyte	6.14	1.32	17.12	18.26	3880	2550	945	465	180	0.24	2.36	1.33	1.60	0.48
Film of Fe and Mn hydroxides on the surface of basalt	2170-2(2)	Si-bearing protoferrihydrite and nontronite	18.37	1.96	35.17	0.72	188	35	48	66	17	0.028	3.46	2.24	2.85	0.53
Socle of hydrothermal mound 1 m high	2170-4	Si-bearing protoferrihydrite and nontronite	15.77	3.20	39.35	1.98	39	26	40	74	10	0.035	1.74	1.04	3.60	0.55

Table 1. (Contd.)

1	2	3	4	5	6	7	8	9	10	11	12	13	14	15	16	17
Upper part of hydrothermal mound 7 m high	2170-7	Si-bearing protoferrihydrite	16.90	2.77	24.92	0.15	12	4.0	14	33	22	0.038	0.90	0.50	3.71	0.47
Fragments carried up from the socle of hydrothermal mound	2192-2(2)a (film on a fragment)	Fe-vernadite and Mn-feroxyhyte	5.76	1.88	18.45	17.85	2750	2310	1500	73	18	0.18	2.56	1.52	1.90	0.38
	2192-2(2)b	Protoferrihydrite and nontronite	11.22	1.60	53.80	0.72	40	70	32	65	14	0.17	2.46	1.22	2.26	0.32
	2192-2(2)c	Nontronite	20.35	0.22	41.26	0.24	94	10	365	805	65	0.13	2.14	0.88	1.78	0.58
Crust on the fragment surface	2192-3	Fe-free vernadite	4.26	0.94	1.45	21.52	670	210	780	350	48	0.21	1.36	1.64	1.86	0.62
Conical hydrothermal mound 5 m high	2202-2A1a	Si-bearing protoferrihydrite, nontronite, and ferrihydrite (small amounts)	19.48	1.65	37.92	0.32	145	65	75	80	30	0.15	1.96	2.08	2.46	0.40
Crust on the surface of the hydrothermal mound	2202-2A1b	Hexagonal bernessite and Fe-free vernadite (small amounts)	1.84	0.47	1.75	20.78	5.40	100	300	145	740	0.175	1.72	1.65	1.63	0.56
Conical hydrothermal mound 2.5 m high	2202-2A2.1 (film up to 1 cm thick on the surface)	Fe-vernadite and Mn-feroxyhyte	5.45	1.06	8.90	26.75	850	447	348	290	10	0.26	2.88	1.36	1.86	0.44
	2202-2A2.2 (1–2 cm)	Si-bearing protoferrihydrite with a high P content (up to 5%) and admixtures of ferrihydrite, hematite, and goethite	8.33	1.64	12.85	6.15	15	20	20	14	7	0.13	3.47	1.44	2.66	0.40
	2202-2A2.3 (2–3 cm)		10.14	1.87	18.66	0.85	4.5	24	12	15	5	0.070	3.72	1.02	2.85	0.30
	2202-2A2.4 (3–4 cm)		11.85	1.98	18.20	0.22	3.5	27	10	12	5	0.11	3.55	1.17	2.34	0.33
Small conical hydrothermal mound	2202-2B2	Bernessite and Fe-free vernadite (small amounts)	1.30	0.55	3.02	26.86	638	125	426	165	210	0.24	3.64	1.76	1.58	0.50
Small hydrothermal mound	2218-6	Protoferrihydrite and hematite	8.04	1.88	41.80	1.30	58	29	125	124	47	0.20	7.24	2.35	5.74	0.44

Table 1. (Contd.)

1	2	3	4	5	6	7	8	9	10	11	12	13	14	15	16	17
Juan de Fuca Ridge, Axial Seamount																
Columnar mounds composed of Fe hydroxides	1491-1	Protoferrihydrite and ferrihydrite	16.90	7.36	50.00	0.28	21	100	47	95	26	0.25	0.29	0.40	1.65	0.20
Film of Fe and Mn hydroxides on the surface of basalt	1479-2a	Fe-vernadite, Mn-feroxyhyte, and goethite (small amounts)	4.77	1.86	39.16	12.86	900	500	100	130	10	0.36	3.50	1.75	1.62	0.22
	1479-2b	Goethite	3.84	2.36	34.74	0.92	120	50	360	160	10	0.17	4.60	2.19	2.20	0.28
	1845-10a	Fe-vernadite, Mn-feroxyhyte, and goethite (small amounts)	2.17	0.74	14.82	18.86	1000	2100	1400	420	820	0.31	1.88	1.64	0.93	0.33
	1845-10b	Fe-free vernadite bernessite (small amounts)	3.27	0.75	0.84	30.52	1585	780	1660	1200	580	0.28	1.96	1.78	1.76	0.57
Small hydrothermal mound	1863-2 (film on the surface)	Fe-vernadite and Mn-feroxyhyte	5.85	1.33	8.72	17.65	1860	1750	945	570	425	0.26	1.86	1.40	1.66	0.44
	1863-4	Protoferrihydrite and hematite (small amounts)	12.45	2.78	48.36	2.64	46	33	155	130	38	0.33	5.18	2.00	3.07	0.40
Thin crust on the surface of basalt	1883-5	Fe-vernadite and Mn-feroxyhyte	9.13	1.44	16.15	19.66	1450	960	1320	1050	775	0.30	3.66	1.47	1.74	0.54
	1883-9	″	10.36	1.08	14.77	16.04	1100	630	1000	820	480	0.22	2.80	1.64	1.43	0.42
Small hydrothermal mound	1891a (film on the surface)	Hematite and ferrihydrite (small amounts)	8.28	1.66	10.24	17.33	1650	1200	1150	980	680	0.36	2.50	1.78	2.06	0.38
	1891b	Fe-vernadite and Mn-feroxyhyte	5.25	0.88	26.82	0.052	10	24	17	20	1.5	0.014	0.84	0.66	1.18	0.15
Thin crust on the surface of basalt	1895	Fe-vernadite and Mn-feroxyhyte	10.80	1.27	15.50	16.85	2720	3885	1500	440	200	0.26	2.27	1.96	1.46	0.45

which contains 6.15 wt % Mn, is the only exception. The Si content in samples ranges mainly from 8.04 to 19.48 wt % and is lower only in goethite (sample 1479-2b) and hematite (sample 1891-b): 3.84 and 5.25 wt %, respectively. The Al contents are 0.88–7.36 wt % in monomineral samples and 1.64–3.20 wt % in samples with Si-bearing protoferrihydrite as the main phase. The contents of heavy metals in Fe minerals are one to two orders of magnitude lower in comparison with Mn minerals.

The third mineral assemblage is composed of practically pure *nontronite* (samples 2157-6, 2157-7, and 2192-2(2)c). In electron microscope specimens, nontronite is observed as fine scaly aggregates. As compared with the above-described nontronite, the mineral under consideration is characterized by a more ordered structure.

The Si content in nontronite ranges from 19.76 to 21.85 wt %. At the same time, these samples show high Fe (40.75–47.14 wt %) and low Al and Mn (0.22–0.32 and 0.24–0.88 wt %, respectively) concentrations (Table 1). The contents of heavy metal cations in the samples are low and comparable with those in protoferrihydrite and Si-bearing protoferrihydrite.

The concentrations of major elements in samples from all examined mineral assemblages vary from tenths of a percent to a few percent (Table 1).

In the opinion of Lisitsyn et al. (1991), the mineral zoning established in low-temperature hydrothermal systems is determined by changes in physicochemical conditions during migration of ore-bearing hydrothermal solution from the central part of the system toward its periphery. Despite the variable modal mineral composition of sediments, their chemical composition is relatively uniform, although the contents of some elements are notably different. For example, concentrations of heavy metals (Cu, Zn, Pb, and others) in hydrothermal minerals vary from thousandths to ten thousandths of a percent (Lisitsyn et al., 1991), while in hydrogenic Fe–Mn minerals their contents are several times or even one to two orders of magnitude higher. Similar proportions were pointed out previously (Bogdanov and Lisitsyn, 1990; Binns et al., 1993; Bogdanov et al., 1997, 2004).

In our opinion, such a significant difference in contents of metals is provided by different rates of nucleation and growth of minerals, primarily Fe hydroxides and Mn oxide–hydroxides, and by different absorptivity of minerals relative to these metals. The absorptive capacity of minerals likely is a crucial factor that controls the chemical composition of low-temperature deposits. Indeed, sorption is the most important process in differentiation of chemical elements, as was shown by experimental studies of oceanic Fe–Mn nodules and crusts of different genesis (Novikov and Yashina, 1993; Novikov, 1996; Novikov and Skornyakova, 1998; Novikov and Cherkashev, 2000).

It is convenient to consider the experimental results for the groups of Fe minerals, Mn minerals, and aluminosilicates separately.

SORPTION OF HEAVY METAL CATIONS ON MINERALS OF LOW-TEMPERATURE DEPOSITS

The study of the ion exchange properties of Fe–Mn deposits may be limited to determination of the main variables (exchange capacity of minerals, composition of exchangeable metal cations, reactivity of these minerals, kinetic parameters of sorption) or to determination of all ion exchange characteristics (Novikov, 2005). As was mentioned above, the examined low-temperature hydrothermal deposits are crusts 1 mm–2 cm thick or films thinner than 2 mm; i.e., the quantity of material was insufficient for determination of all ion exchange parameters and compelled us to limit ourselves to the main characteristics. Nevertheless, the results obtained make it possible to characterize low-temperature hydrothermal deposits of different mineral compositions as natural ion exchangers in comparison with Fe–Mn deposits of diagenetic and sedimentary origins.

Concentrated (1 N) solutions of heavy metal salts were used in order to determine the maximal possible absorptivity (exchange capacity) of low-temperature hydrothermal mineral assemblages under given physicochemical conditions. The use of such highly concentrated solutions was dictated primarily by kinetic reasons. Second, the composition of the exchange complex of minerals was established simultaneously with the determination of the exchange capacity. Third, the effect of other (in addition to those examined) dissolved metal cations (except protons H^+) on the solid phase is practically ruled out. Such an approach allowed all obtained data to be interpreted from the same standpoint despite the different mineral composition of examined samples. Recall that highly concentrated solutions have repeatedly been used for the study of the ion exchange properties of other natural minerals, e.g., micas, clays, zeolites, alkali feldspars, and sulfides (Deer et al., 1962; Zaitseva, 1966; Chelishchev, 1973; Tarasevich and Ovcharenko, 1975; Breck, 1973; Chelishchev et al., 1988). Interpretation of the obtained results took into account that exchange reactions proceed primarily on dominant mineral phases of each sample and the ion exchange properties of particular minerals are controlled by the structural type of lattice and the position of metal cations therein. The comparison of data on sorption of metal cations from solutions with concentrations of 1.0–0.001 N offers the opportunity to consider the mechanism responsible for their concentration in minerals of low-temperature hydrothermal deposits.

Interaction of samples of different mineral compositions and genesis with water solutions of metal salts results in modification of the chemical composition of

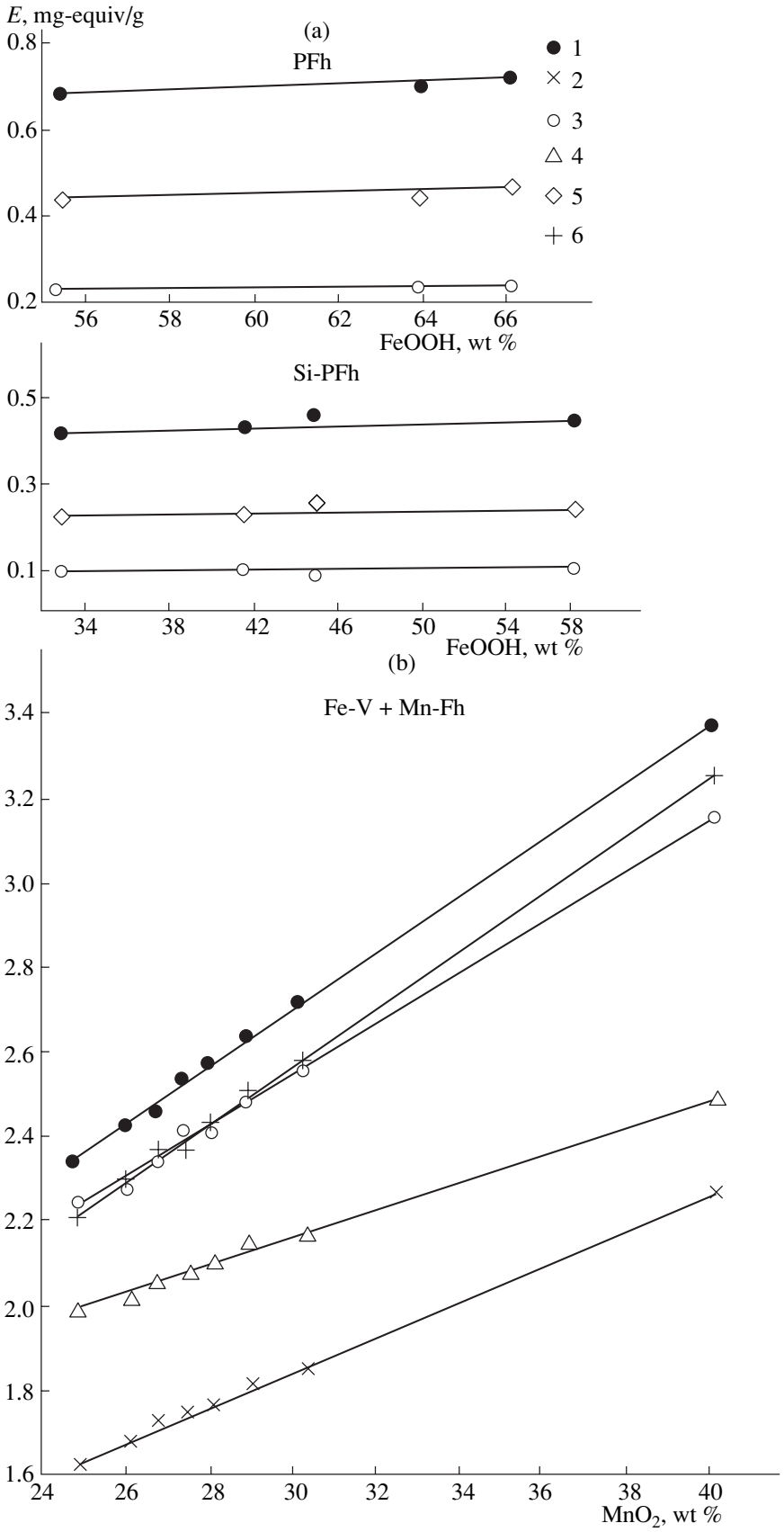

Fig. 2. Exchange capacity of (a) Fe and (b, c) Mn minerals versus FeOOH and MnO_2 contents in samples, respectively. Absorbed cations: (1) Cu, (2) Co, (3) Zn, (4) Ni, (5) Mn, and (6) Pb.

the samples, which become enriched in alkali and alkali-earth metals (first of all) and depleted in heavy metals. Hence, exchange reactions between metal cations proceed in all examined heterogeneous systems. The exchange between cations depends on the modal composition and crystallochemical properties of minerals, the nature of absorbed cations, and other parameters. Thereby, the exchange capacity of minerals (and their assemblages) is highly variable. Let us consider the data on sorption of metal cations for each of the aforementioned mineral assemblages from low-temperature hydrothermal deposits.

The absorptive capacity of *Fe minerals* varies from 0.03 to 0.98 mg-equiv/g, with maximal (0.44–0.98 mg-equiv/g) and minimal (0.03–0.28 mg-equiv/g) values characteristic of goethite and hematite, respectively (Table 2). In general, the sorption activity of Fe minerals increases in the following order:

hematite < Si-bearing protoferrihydrite < protoferrihydrite < goethite.

The low exchange capacity of hematite is explained by its belonging to the minerals with a coordination-type structure, which is characterized by a very compact arrangement of atoms in the lattice, while the other Fe minerals pertain to minerals with a layer structure.

Hematite from sample 1891-b (Figs. 1e, 1f) is characterized by a low exchange capacity relative to all heavy metals (0.03–0.28 mg-equiv/g) irrespective of the concentration of their solutions (Table 3). These values are comparable with similar data obtained by Novikov and Cherkashev (2000) despite the fact that the Fe contents in hematite were different: 26.82 wt % in our sample and 15.20 wt % in the material used in the cited publication. The exchange of all heavy metal cations except Cu^{2+} on hematite occurs at the expense of Na^+; in the case of Cu^{2+}, it occurs at the expense of Na^+ and Ca^{2+} (Table 4). Thereby, the exchange between metal cations of the solid and liquid phases is equivalent. The pH values in equilibrium solutions also remained unchanged relative to the initial values (Table 5).

The exchange capacity of protoferrihydrite (samples 1491-1, 1863-4, and 2218-6) and Si-bearing protoferrihydrite (samples 2157-10, 2157-11, 2157-14, and 2170-7) with respect to heavy metal cations absorbed from 1 N solutions ranges from 0.23 to 0.74 and from 0.10 to 0.48 mg-equiv/g, respectively (Table 2). The data obtained show that the exchange capacity of protoferrihydrite relative to all cations is 1.5–2 times higher in comparison with Si-bearing protoferrihydrite, probably, owing to the structural and textural properties of the latter. Furthermore, the exchange capacity of protoferrihydrite and its siliceous variety relative to each examined element is practically constant and is independent of the Fe^{3+} (FeOOH) content in samples (Fig. 2a). This indicates that the number of exchange centers in minerals is limited and these minerals achieved their maximal exchange capacity under the physicochemical conditions of the experiment.

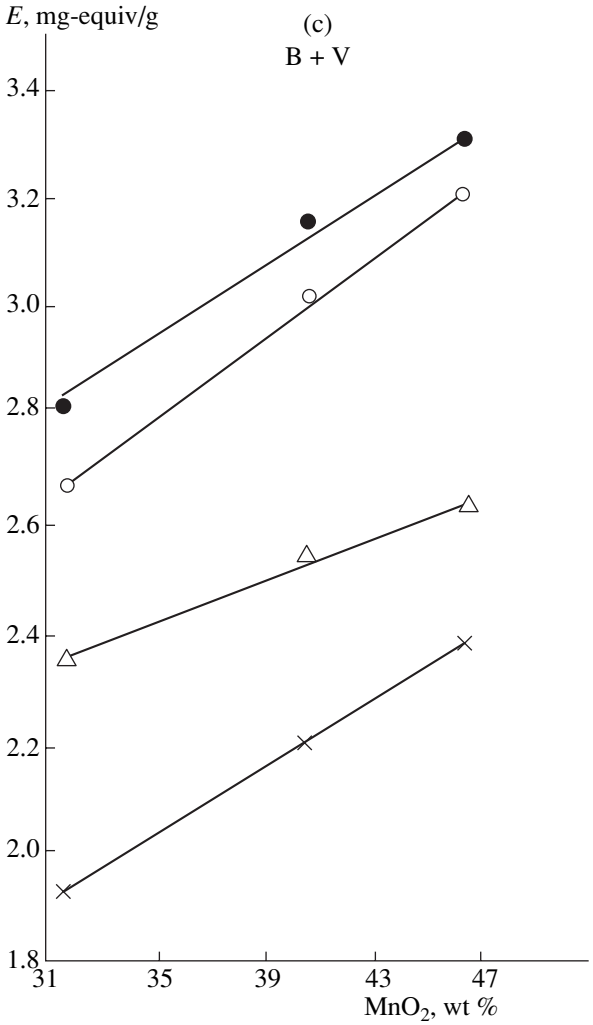

Fig. 2. (Contd.)

The absorptivity of both minerals is realized by passage of cations of major elements (Na^+, K^+, Ca^{2+}, and Mg^{2+}) (Table 2, sample 1491-1) into solution; the reactivity of these elements (mg-equiv/g) decreases in the following order: Na > Mg ⩾ Ca > K. At the same time, all examined samples demonstrate the prevalence of the sum of removed metal cations over the quantity of absorbed metal cations, with an increase in the pH of equilibrium solutions by 0.20–0.35 units relative to the pH of initial solutions (Table 5). This implies that Fe minerals also absorb protons H^+ in addition to heavy metal cations.

At the same time, the results obtained for the sorption of heavy metal cations from solutions with lower concentrations (0.1–0.001 N) demonstrate a decrease in the exchange capacity of both minerals relative to the values presented in Table 2. Their exchange capacity decreased by 0.04–0.11 mg-equiv/g in the case of 0.1 N solutions and amounts only to 0.02–0.11 mg-equiv/g in the case of their sorption from 0.001 N solutions (Table 3, samples 1491-1 and 2157-10). The decrease in the

Table 2. Exchange capacity, mg-equiv/g of low-temperature hydrothermal and hydrogenic deposits (concentration of solution equals 1 N)

Sample number	Mineral assemblage	Absorbed cation							Series of increasing capacity
		Mn	Ni	Co	Cu	Zn	Cd	Pb	
1	2	3	4	5	6	7	8	9	10
1891b	H and Fh (small amounts)	0.04	0.07	0.04	0.28	0.08	0.03	0.12	Cd, Mn, Co < Ni, Zn < Pb < Cu
1491-1	PFh and Fh	0.28	0.31	0.26	0.74	0.48	0.34	0.70	
1863-4	PFh and H (small amounts)	0.27	0.29	0.25	0.72	0.45	0.34	0.70	
2218-6	″	0.25	0.27	0.23	0.68	0.44	0.32	0.63	
Average		0.26	0.29	0.24	0.71	0.45	0.33	0.67	Co < Mn < Ni < Cd < Zn < Pb < Cu
2192-2(2)b	PFh and N	0.31	0.54	0.38	0.95	0.50	0.60	0.91	Mn < Co < Zn < Ni < Cd < Pb < Cu
2157-10	Si-PFh	0.16	0.15	0.13	0.47	0.26	0.18	0.42	
-11	″	0.12	0.16	0.11	0.45	0.24	0.16	0.42	
-14	″	0.14	0.17	0.10	0.48	0.26	0.18	0.43	
2170-7	″	0.10	0.16	0.10	0.42	0.23	0.14	0.40	
Average		0.13	0.16	0.11	0.45	0.25	0.17	0.42	Co < Mn < Ni, Cd < Zn < Pb < Cu
2202-2A2.2	Si-PFh, Fh, G, and H (small amounts except Si-PFh)	0.36	0.31	0.68	0.80	0.33	0.34	0.77	
-2A2.3		0.14	0.18	0.13	0.51	0.22	0.16	0.42	
-2A2.4		0.14	0.16	0.12	0.44	0.22	0.16	0.42	
2170-2(2)	Si-PFh and N	0.23	0.33	0.19	0.62	0.30	0.38	0.57	
-4	″	0.28	0.34	0.24	0.66	0.31	0.39	0.55	
2202-2A1a	Si-PFh, N, and Fh	0.24	0.36	0.23	0.70	0.34	0.41	0.63	
Average		0.23	0.34	0.26	0.62	0.32	0.39	0.56	Mn < Co < Zn < Ni < Cd < Pb < Cu

Table 2. (Contd.)

1	2	3	4	5	6	7	8	9	10
1479-2b	H	0.44	0.52	0.56	0.98	0.58	0.72	0.94	Mn < Ni < Co < Zn < Cd < Pb < Cu
2157-6	N	0.36	1.17	1.06	1.19	0.39	1.23	1.26	
2192-2(2)c	N	0.34	1.14	1.10	1.20	0.37	1.26	1.30	
2157-7	N and PFh (small amounts)	0.38	1.18	1.04	1.24	0.43	1.24	1.30	
Average		0.36	1.16	1.06	1.21	0.40	1.24	1.28	Mn < Zn < Co < Ni < Cu < Cd < Pb
2192-3	V	2.42	2.08	2.75	2.97	2.20	2.24	2.83	
2202-2A1b	B + V	2.36	1.92	2.66	2.80	2.08	2.07	2.72	
2202-2B2		2.54	2.20	3.02	3.14	2.36	2.41	3.05	
1845-10b		2.63	2.38	3.20	3.30	2.48	2.54	3.23	
Average		2.51	2.16	2.96	3.08	2.30	2.34	3.00	
2157-14a	B	2.97	2.60	3.48	3.58	2.73	2.78	3.52	
1479-2a	Fe-V + Mn-Fh	1.84	1.42	1.97	1.95	1.70	1.73	1.88	
1883-9		2.00	1.62	2.24	2.31	1.83	1.88	2.21	
1895		2.02	1.66	2.28	2.42	1.85	1.92	2.29	
1891a		2.06	1.70	2.34	2.46	1.90	1.96	2.36	
1863-2		2.08	1.72	2.37	2.49	1.91	1.97	2.36	
2192-2(2)a		2.08	1.73	2.39	2.52	1.93	1.97	2.38	
2170-2(1)		2.10	1.74	2.41	2.56	1.94	1.98	2.41	
1845-10a		2.14	1.80	2.48	2.63	1.96	1.96	2.49	
1883-5		2.16	1.84	2.55	2.70	2.03	2.08	2.57	
2202-2A2.1		2.47	2.24	3.13	3.35	2.30	2.27	3.22	
Average		2.12	1.78	2.47	2.54	1.96	2.00	2.48	Ni < Zn < Cd < Mn < Co < Pb < Cu

Note: Here and in Tables 4–6: (B) bernessite; (V and Fe-V) Fe-free and Fe-vernadite; (G) goethite; (H) hematite; (N) nontronite; (Fh, PFh, and Si-PFh) ferrihydrite, protoferrihydrite, and Si-bearing protoferrihydrite; (Mn-Fh) Mn-feroxyhyte.

Table 3. Exchange capacity, mg-equiv/g, of low-temperature hydrothermal and hydrogenic deposits versus concentrations of metal salt solutions

Sample numbe	Solution concentration, N	Absorbed cation			
		Mn	Ni	Co	Cu
1883-5	1.0	2.16	1.84	2.55	2.70
	0.1	2.06	1.74	2.44	2.58
	0.01	1.95	1.63	2.31	2.50
	0.001	0.98	0.92	1.30	1.45
2202-2B2	1.0	2.64	2.20	3.04	3.14
	0.1	2.50	2.04	2.90	3.06
	0.01	2.28	1.80	2.68	2.84
	0.001	0.94	0.88	1.32	1.38
2157-14a	1.0	2.97	2.60	3.36	3.58
	0.01	2.66	2.23	3.00	3.23
	0.001	1.24	1.16	1.57	1.76
1479-2b	1.0	0.44	0.52	0.56	0.98
	0.1	0.36	0.40	0.41	0.88
	0.001	0.08	0.08	0.05	0.12
1891b	1.0	0.04	0.07	0.04	0.28
	0.01	0.02	0.03	0.01	0.12
	0.001	0.02	0.02	0.01	0.05
1491-1	1.0	0.28	0.31	0.26	0.74
	0.1	0.22	0.24	0.22	0.65
	0.01	0.10	0.15	0.10	0.48
	0.001	0.03	0.06	0.04	0.11
2157-10	1.0	0.14	0.15	0.13	0.47
	0.1	0.11	0.11	0.09	0.35
	0.01	0.06	0.06	0.04	0.21
	0.001	0.03	0.04	0.03	0.10
2157-6	1.0	0.36	1.17	1.06	1.19
	0.1	0.22	1.03	0.96	1.10
	0.01	0.10	0.82	0.68	0.92
	0.001	0.04	0.30	0.16	0.23

exchange capacity of minerals with respect to heavy metal cations results in a reduced difference between the exchange capacity and the sum of removed exchange cations. In the case of sorption of heavy metal cations from 0.001 N solutions, this difference is negligible; i.e., the exchange is equivalent (Table 4, sample 1491-1). This is supported by a similar pH of the equilibrium and initial solutions (Table 5). Hence, the exchange capacity of protoferrihydrite and Si-bearing protoferrihydrite is realized only at the expense of their exchange cations, while protons H^+ do not participate in these reactions.

The presence of several mineral phases in samples changes their absorptive properties. For example, the occurrence of nontronite in sample 2192-2(2)b, in addition to protoferrihydrite, increases the exchange capacity by 0.06 mg-equiv/g with respect to Mn and Zn and by 0.24–0.27 mg-equiv/g with respect to Cu, Pb, Ni, and Cd as compared with "pure" protoferrihydrite. A similar situation is characteristic also of Si-bearing protoferrihydrite, as is evident from a comparison of data on the respective samples (Table 2).

As was mentioned above, goethite, a mineral of sedimentary genesis, is characterized by the highest absorptive capacity among the Fe minerals. Despite their different origin, the ion exchange reactions on goethite are similar to those on other Fe minerals. According to the data on sorption of metal cations from 1.0–0.1 N solutions, the exchange capacity of goethite increases from Mn to Cu and then to Pb. The exchange

Table 4. Chemical composition of low-temperature hydrothermal deposits after sorption of heavy metal cations thereon

Sample number (mineral assemblage)	Cation species	Concentration (N) of M^{2+} salt solutions	Content of cations M^{2+}, 10^{-4} wt %					Content of cations M^{n+}, wt %					Sum of removed M^{n+}	Exchange capacity
			Ni	Co	Cu	Zn	Pb	Mn^{2+}	Ca	Mg	Na	K	mg-equiv/g	
1	2	3	4	5	6	7	8	9	10	11	12	13	14	15
1479-2b (G)	Initial*	–	120	50	360	160	10	0.27	4.60	2.19	2.20	0.28	–	–
	Mn	1.0	116	50	346	155	10	1.48	1.88	1.98	1.58	0.16	0.69	0.44
		0.001	120	50	357	158	10	0.49	4.52	2.16	2.10	0.24	0.11	0.08
	Ni	1.0	15400	48	340	153	10	0.13	4.14	2.02	1.55	0.16	0.73	0.52
		0.001	2400	48	355	156	10	0.21	4.52	2.16	2.10	0.24	0.13	0.08
	Co	1.0	108	16500	335	154	8.5	0.05	4.16	2.04	1.55	0.20	0.72	0.56
		0.001	114	1500	340	158	9	0.19	4.56	2.18	2.13	0.24	0.09	0.05
	Cu	1.0	102	45	31500	150	8.5	0.10	3.80	1.93	1.12	0.05	1.20	0.98
		0.001	114	47	4200	157	9	0.21	4.54	2.16	2.06	0.24	0.14	0.12
1491-1 (PFh, Fh)	Initial	–	21	100	47	95	26	0.28	0.29	0.40	1.65	0.20	–	–
	Mn	1.0	20	94	42	87	26	1.05	0.17	0.20	1.21	0.12	0.43	0.28
		0.001	20	96	46	92	26	0.37	0.27	0.38	1.60	0.16	0.05	0.03
	Ni	1.0	9100	94	40	90	24	0.20	0.17	0.22	1.14	0.12	0.48	0.31
		0.001	1800	95	43	94	25	0.27	0.27	0.37	1.58	0.16	0.07	0.06
	Co	1.0	18	7700	37	90	23	0.09	0.17	0.24	1.26	0.12	0.45	0.26
		0.001	20	1200	43	94	24	0.20	0.25	0.37	1.58	0.16	0.11	0.04
	Cu	1.0	17	88	23600	86	22	0.14	0.05	0.22	0.48	0.02	0.88	0.74
		0.001	19	92	3500	90	24	0.25	0.27	0.36	1.51	0.16	0.12	0.11
2157-6 (N)	Initial	–	54	37	140	164	24	0.26	2.76	1.86	5.64	0.42	–	–
	Mn	1.0	52	35	135	162	23	1.25	2.46	1.70	5.13	0.26	0.53	0.36
		0.001	52	37	138	162	23	0.37	2.72	1.85	5.59	0.42	0.04	0.04
	Ni	1.0	34300	33	136	150	22	0.04	1.84	1.68	4.40	0.11	1.30	1.17
		0.001	8800	34	138	158	23	0.17	2.58	1.81	5.32	0.34	0.32	0.30
	Co	1.0	50	31300	135	156	23	0.01	1.80	1.70	4.33	0.15	1.33	1.06
		0.001	52	4700	137	160	23	0.09	2.68	1.84	5.48	0.38	0.19	0.16
	Cu	1.0	48	33	37900	140	21	0.04	1.76	1.68	4.26	0.07	1.41	1.19
		0.001	51	35	7400	150	23	0.17	2.62	1.82	5.36	0.34	0.27	0.23

Table 4. (Contd.)

1	2	3	4	5	6	7	8	9	10	11	12	13	14	15
2157-14 a (B)	Initial	–	956	307	343	288	62	1.53	2.40	1.84	2.06	0.72	–	–
	Mn	1.0	940	303	338	276	60	9.70	0.04	0.90	0.06	0.10	2.98	2.97
		0.001	952	305	338	284	62	4.94	1.04	1.77	1.07	0.45	1.24	1.24
	Ni	1.0	76400	298	337	275	60	0.92	0.08	1.42	0.08	0.13	2.74	2.60
		0.001	34100	303	340	285	62	1.42	1.16	1.78	1.12	0.52	1.17	1.16
	Co	1.0	933	99000	330	270	50	0.01	0.06	1.33	0.06	0.10	3.17	3.36
		0.001	950	46300	340	280	58	0.87	1.00	1.75	0.96	0.45	1.56	1.57
	Cu	1.0	930	294	113900	270	50	0.10	0.04	1.20	0.03	0.10	3.27	3.58
		0.001	947	300	56000	280	60	0.98	0.84	1.71	0.82	0.33	1.72	1.76
2192-3 (V)	Initial	–	670	210	780	350	48	0.77	1.36	1.64	1.86	0.62	–	–
	Mn	1.0	655	195	765	330	48	6.94	0.04	0.77	0.04	0.08	2.30	2.42
		0.001	670	200	780	345	48	3.85	0.40	1.40	0.62	0.40	1.28	1.30
	Ni	1.0	49000	205	760	340	48	0.44	0.04	0.88	0.04	0.08	2.32	2.08
		0.001	36800	210	780	345	48	0.60	0.42	1.45	0.68	0.43	1.24	1.25
	Co	1.0	615	81000	755	330	42	0.01	0.02	0.86	0.04	0.08	2.52	2.75
		0.001	650	43700	775	345	45	0.03	0.38	1.49	0.64	0.43	1.46	1.48
	Cu	1.0	600	185	94500	320	40	0.08	0.02	0.82	0.04	0.04	2.57	2.97
		0.001	650	200	50300	340	45	0.16	0.28	1.44	0.55	0.27	1.58	1.58
1883-5 (Fe-V and Mn-Fh)	Initial	–	1450	960	1320	1050	775	0.50	3.66	1.47	1.74	0.54	–	–
	Mn	1.0	1400	930	1290	950	760	6.44	2.60	0.96	0.08	0.11	2.28	2.16
		0.001	1425	950	1310	1000	770	3.20	2.80	1.25	0.98	0.38	0.98	0.98
	Ni	1.0	56500	950	1290	1000	765	0.30	2.60	1.09	0.13	0.15	2.21	1.84
		0.001	28500	955	1315	1025	770	0.44	2.78	1.32	1.05	0.38	0.92	0.92
	Co	1.0	1365	75200	1275	935	750	0.01	1.58	1.04	0.06	0.15	2.40	2.55
		0.001	1400	38400	1300	990	765	0.06	2.70	1.30	0.77	0.23	1.28	1.30
	Cu	1.0	1350	920	86000	935	750	0.06	2.56	1.00	0.06	0.02	2.46	2.70
		0.001	1390	940	46200	980	760	0.11	2.62	1.22	1.63	0.11	1.45	1.45

* Contents of heavy metal cations in initial sample correspond to Table 1.

Table 5. Average pH of equilibrium solutions after sorption of heavy metal cations on low-temperature hydrothermal deposits

Solution of metal salt	pH of initial solution with concentration, N		Average pH of equilibrium solutions with concentrations, N															
	1.0	0.001	1.0	0.001	1.0	0.001	1.0	0.001	1.0	0.001	1.0	0.001	1.0	0.001	1.0	0.001	1.0	0.001
	1.0	0.001	B		V		B and V		Fe-V and Mn-Ph		G		PFh and Si-PFh		H		N	
$MnCl_2$	4.80	6.45	4.90	6.45	5.10	6.40	5.20	6.50	4.95	6.50	5.10	6.50	4.95	6.45	4.85	6.45	5.05	6.45
$Ni(NO_3)_2$	3.80	6.50	4.00	6.50	4.35	6.50	4.35	6.55	4.15	6.50	4.20	6.50	4.00	6.50	3.80	6.50	4.00	6.55
$Co(NO_3)_2$	3.45	6.60	3.05	6.45	3.10	6.50	3.30	6.50	3.00	6.55	3.90	6.60	3.75	6.65	3.45	6.60	3.65	6.60
$Cu(NO_3)_2$	3.40	5.20	3.00	5.05	2.95	5.15	3.20	5.20	3.10	5.25	3.80	5.25	3.60	5.25	3.45	5.25	3.55	5.30
$ZnSO_4$	4.20	6.30	4.50	6.35	4.60	6.30	4.70	6.35	4.40	6.40	4.65	6.35	4.40	6.30	4.20	6.30	4.40	6.35
$Cd(NO_3)_2$	5.20	6.30	5.40	6.30	5.65	6.30	5.60	6.35	5.45	6.30	5.45	6.30	5.45	6.30	5.30	6.30	5.35	6.30
$Pb(NO_3)_2$	3.70	5.60	3.25	5.40	3.40	5.50	3.55	5.55	3.35	5.85	4.10	5.65	3.95	3.80	3.65	5.65	3.90	5.65

capacity for these elements differs more than twofold, indicating selective absorptivity (Tables 2, 3). Exchange reactions in goethite are accompanied by passage of cations of alkali and alkali-earth metals into solutions (Table 4, sample 2157-6); their exchange capacity decreases in the following order irrespective of absorbed heavy metal cations: Na > Ca > Mg > K. As in the case of protoferrihydrite and its siliceous variety, the pH of equilibrium solutions is higher by 0.20–0.45 units than the pH of initial solutions (Table 5). This means that goethite is able to absorb from solutions not only heavy metal cations but also protons H^+; as a result, the exchange remains equivalent and the mineral matrix is electrically neutral.

Goethite is characterized by the same relationships typical of other Fe minerals: the exchange capacity decreases with reduced concentration of metal cations in solutions, the sum of removed exchange cations is equal to the capacity for the respective cation of heavy metal, and the pH remains equal in the initial and equilibrium solutions (Tables 3–5).

The trends of increasing exchange capacity of Fe minerals with respect to the examined elements are practically identical (Table 2) and thus indicate that the ion exchange properties of these minerals are close to one another. By capacity values, the metals may conditionally be divided into three groups. In the case of protoferrihydrite, Si-bearing protoferrihydrite, and polymineral samples, the first group consists of Mn and Co and the third group of Pb and Cu, and they are characterized by minimal and maximal capacity values, respectively. Cu always occupies the extreme right position, while Co and Mn can change places in the succession. The second group comprises Ni, Cd, and Zn, which occupy an intermediate position between elements of the first and third groups. As concerns hematite and goethite, the succession is changed. In the case of hematite, Cd is placed into a common group with Co and Mn, while, in the case of goethite, Cd may be regarded as an autonomous group and, thus, the following succession is established: Mn, Ni, Co, and Zn (the first group); Cd (the second group); and Pb and Cu (the third group).

The absorptivity of *nontronite* (samples 2157-6, 2157-7, and 2192-2(2)c) is substantially higher than that of Fe minerals owing to its lattice structure and physicochemical properties. Two types of isomorphic replacements are characteristic of nontronite: Si^{4+} with Al^{3+} in the octahedral layer and Si^{4+} with Fe^{3+} in the tetrahedral layer. In addition, Mg^{2+} and, probably, an insignificant quantity of Fe^{3+}, Mn^{2+}, and Ni^{2+} are also contained in octahedral coordination (Deer et al., 1962). These replacements result in the appearance of a negative charge in the Al–Si–O framework of the mineral that is compensated by interlayer cations, primarily by Na^+ and Ca^{2+}, which provide the ion exchange properties of nontronite.

The results of exchange reactions indicate a selective capacity of nontronite with respect to heavy metal cations. Based on exchange capacity (sorption of cations from 1.0 N solutions), the metals are divided into two groups. The first group consists of Mn and Zn, which show the minimal capacity (0.34–0.38 and 0.37–0.43 mg-equiv/g, respectively). The remaining heavy metals, whose capacity varies from 1.04 to 1.30 mg-equiv/g (Table 2), are included in the second group. These relationships are reflected in the series of progressive growth of the exchange capacity inherent to nontronite (Table 2).

The exchange complex of nontronite consists of the same cations as that of Fe minerals: Na^+, K^+, Ca^{2+}, and Mg^{2+} (Table 4, sample 2157-6). Their reactivity decreases in the following order: Na > Ca > Mg > K. The contribution of each exchange cation to the total capacity of the mineral decreases in the same direction. Like Fe minerals, nontronite also absorbs protons H^+ in addition to heavy metal cations: the pH of equilibrium solutions increases by 0.15–0.25 units relative to the pH of initial solutions (Table 5). This implies that, during

sorption of heavy metal cations from concentrated solutions, only exchange cations of nontronite take part in the exchange reaction, while protons H^+ play a subordinate role in this process. In the case of 0.001 N solutions, sorption is provided only at the expense of exchange cations contained in nontronite, as is confirmed by the pH of equilibrium solutions (Tables 4, 5). Nontronite is characterized by the same relationship as that for Fe minerals: a decrease in the concentration of heavy metal cations in solutions results in a decreased exchange capacity (Table 3, sample 2157-6).

Our data on nontronite absorptivity are in rather good agreement with the values obtained for minerals of the montmorillonite group (0.80–1.50 mg-equiv/g) by Deer et al. (1962), Kokotov (1980), and Zuzuk and Kryukov (1987).

In exchange capacity, hydrothermal *Mn minerals* substantially exceed not only the studied Fe minerals and aluminosilicates of the same genesis but also hydrogenic Mn minerals (Table 2). The following order of Mn minerals is established in accordance with increasing exchange capacity with respect to all metals: Fe-vernadite, Mn-feroxyhyte < vernadite < bernessite + vernadite < bernessite.

The exchange capacity of the hydrothermal assemblage Fe-vernadite + Mn-feroxyhyte + Mn minerals (by sorption of metal cations from 1.0–0.1 N solutions) varies within the same limits as in samples of similar composition studied by Chelishchev et al. (1992), Novikov and Yashina (1993), Novikov et al. (1995), Novikov (1996), and Novikov and Cherkashev (2000). The obtained capacities of Mn minerals with respect to all heavy metal cations are high for natural inorganic ion exchangers and indicate that these metals are absorbed by the entire crystallochemical volume of the Mn minerals. The same was noted previously for diagenetic and sedimentary–diagenetic nodules composed of various Mn minerals with a layer structure. The character of exchange reactions that proceed with participation of Mn minerals is similar regardless of their genesis, so that the obtained results may be described in general terms.

A direct correlation between the exchange capacity and the content of quadrivalent Mn (MnO_2) was established for hydrogenic crusts composed of Fe-vernadite and Mn-feroxyhyte (Fig. 2b). Similar results were obtained for other samples of sedimentary crusts from various areas of the World Ocean (Novikov and Yashina, 1993; Novikov, 1996). A direct correlation was also established for low-temperature hydrothermal deposits composed of bernessite and vernadite (samples 2202-2A1b, 2202-2B2 and 1845-10b) (Fig. 2c).

However, the absorptivity of samples is determined not only by the content of MnO_2 but also by their mineral compositions, as is evident from a comparison of the exchange capacity obtained for samples 2157-14a and 1845-10b. The first sample is composed exclusively of bernessite, while the second sample consists of vernadite and subordinate bernessite. The Mn contents in these samples are practically identical: 30.52 and 30.84 wt %, respectively (Table 1). At the same time, the absorptive capacity of sample 2157-14a with respect to various heavy metal cations is by 0.22–0.34 mg-equiv/g higher than that of sample 1845-10b (Table 2).

The absorptivity of all examined Mn minerals increases in the same succession from Ni^{2+} toward Cu^{2+}. In each mineral assemblage, the arrangement of metal cations in this succession is similar and allows compiling of a common series (Table 2). By exchange capacity, metals are divided into two groups: (1) Ni^{2+}, Zn^{2+}, Cd^{2+}, and Mn^{2+} and (2) Co^{2+}, Pb^{2+}, and Cu^{2+}.

In addition to Na^+, K^+, Ca^{2+}, and Mg^{2+}, the exchange complex of all Mn minerals also includes cations of heavy metals: Mn^{2+}, Cu^{2+}, Ni^{2+}, Co^{2+}, and Ba^{2+}. However, only the contribution of Mn^{2+} to the exchange capacity of Mn minerals is substantial, reaching 0.46–0.55 mg-equiv/g for samples 1845-10b, 2157-14a, 2202-2A2.1, and 2202-2B2. The total contribution of other heavy metal cations to the total capacity of Mn minerals does not exceed 0.05 mg-equiv/g. Among the main exchange cations, the highest reactivity is characteristic of Ca^{2+} and Na^+ and the lowest, of K^+ (Table 4). The series of decreasing reactivity of metal cations and their contribution to the exchange capacity of Mn minerals coincide: Ca > Na > Mg > Mn^{2+} > K > (Ba, Ni, Zn, Cu, Co).

Two specific features of absorption of heavy metal cations by Mn minerals of low-temperature hydrothermal deposits have been revealed. First, the character of absorption of metal cations by Mn minerals belonging to the first and the second groups is different irrespective of their genesis. The sum of cations from the exchange complex of Mn minerals passing into solution is higher by 0.14–0.37 mg-equiv/g than the amount of absorbed Ni^{2+}, Zn^{2+}, Cd^{2+}, and Mn^{2+} (the first group of cations). At the same time, the exchange capacity of these minerals with respect to Co^{2+}, Pb^{2+}, and Cu^{2+} (the second group) exceeds by 0.15–0.30 mg-equiv/g the quantity of removed cations of the exchange complex, Mn^{2+} included (Table 4). The exchange equivalency is retained in the first case owing to sorption of protons H^+ by Mn minerals, and in the second case, by passage of protons that occupy certain positions in Mn minerals into solution. Correspondingly, sorption is accompanied by an increase in the pH of equilibrium solutions by 0.20 units (on average) relative to the pH of initial solutions in the case of metal cations belonging to the first group and by a decrease in the pH by 0.40–0.55 units in the case of metal cations of the second group (Table 5). This means that protons H^+ enter into the exchange complex of Mn minerals during sorption of Co^{2+}, Cu^{2+}, and Pb^{2+}.

The second specific feature of exchange reactions is related to sorption of Co^{2+}, which is accompanied by

Table 6. Enrichment coefficients of mineral assemblages after sorption of heavy metal cations

Ratio of mineral assemblages	Absorbed cation						
	Mn	Ni	Co	Cu	Zn	Cd	Pb
(Fe-V + Mn-Fh) : G	4.82	3.42	4.41	2.59	3.38	2.78	2.64
(Fe-V + Mn-Fh) : H	53.0	25.4	61.8	9.07	24.5	66.6	19.1
(Fe-V + Mn-Fh) : PFh	7.57	5.09	7.97	3.58	4.17	5.00	3.70
(Fe-V + Mn-Fh) : Si-PFh	16.3	11.1	22.4	5.64	7.84	11.7	5.90
(Fe-V + Mn-Fh) : N	5.89	1.53	2.47	2.10	4.90	1.61	1.94
V : G	5.50	4.00	4.91	3.03	3.79	3.11	3.01
V : H	60.5	29.7	68.8	10.6	27.5	74.6	23.6
V : PFh	9.31	7.17	11.5	4.18	4.89	6.79	4.22
V : Si-PFh	18.6	13.0	25.0	6.60	8.80	13.2	6.74
Be : N	6.72	1.78	2.75	2.45	5.50	1.80	2.21
B : G	6.75	5.00	6.21	3.65	4.71	3.86	3.74
B : H	74.2	37.1	86.5	12.8	34.1	92.6	27.1
B : PFh	10.6	7.43	11.1	4.65	5.81	6.95	4.82
B : Si-PFh	22.8	16.2	31.4	7.96	10.9	16.4	8.38
B : N	8.25	7.22	3.48	2.96	6.82	2.24	2.75
B : G	0.82	2.23	1.79	1.23	0.69	1.72	1.36
B : H	9.00	16.6	25.0	4.32	5.00	41.3	10.6
N : PFh	1.38	4.00	4.16	1.70	0.89	3.76	1.91
N : Si-PFh	2.77	7.25	9.09	2.69	1.60	7.29	3.05

the complete removal of Mn^{2+} from hydrothermal Mn minerals, whereas, during sorption of Cu^{2+} and Pb^{2+}, only 88.8–94.5% of divalent Mn is removed. Sorption of other cations of heavy metals is accompanied by much lesser removal of Mn^{2+}, which does not exceed 35.8–43.7% of its initial content in samples (Table 4). Such a character of the exchange reaction $Co^{2+}_{solution} + Mn^{4+}_{solid} \longrightarrow Co^{2+}_{solid} + Mn^{2+}_{solution}$ was previously pointed out for layer Mn minerals from diagenetic and sedimentary nodules, crusts, and crustal–nodular deposits (Chelishchev et al., 1992; Novikov and Yashina, 1993; Novikov and Skornyakova, 1998). Now, this phenomenon has been established also for low-temperature hydrothermal Mn minerals. Hence, it may be stated that this relationship is characteristic of all layer Mn minerals irrespective of their genesis.

A decreased concentration of heavy metal cations in solutions leads to a differential reduction in the exchange capacity of Mn minerals irrespective of their origin. When cations are absorbed from 0.1 and 0.01 N solutions, the exchange capacity of Mn minerals decreases by 0.08–0.14 and 0.20–0.40 mg-equiv/g, respectively, in comparison with absorption from 1.0 N solutions. In the case of absorption of metal cations from 0.001 N solutions, the capacity is as high as 0.83–1.76 mg-equiv/g, i.e., equals 35–54% of its maximal value (Tables 3, 4). The exchange capacity of Mn minerals remains high for natural absorbents and exceeds the capacity of Fe minerals and nontronite observed during absorption of metal cations from concentrated (1.0–0.1 N) solutions.

The exchange reactions with participation of Mn minerals revealed one more specific feature of heavy metal absorption. The exchange capacity of Mn minerals with respect to Ni^{2+}, Zn^{2+}, and Cd^{2+} absorbed from 1.0–0.01 N solutions is always lower than the quantity of removed exchange cations. As concerns Mn^{2+}, Co^{2+}, Cu^{2+}, and Pb^{2+}, the capacity is, conversely, higher. In the case of sorption from 0.001 N solutions, these values are either equal or close to equality for all metal cations (Table 4). The pH of equilibrium solutions (1.0–0.01 N) of Ni, Zn, and Cd salts is by 0.10–0.55 units higher than the pH of initial solutions, whereas the pH of equilibrium solutions of Co, Cu, and Pb salts is by 0.15–0.45 units lower. In the case of sorption of heavy metal cations from 0.001 N solutions, the pH values of equilibrium and initial solutions are either equal or have a difference approaching zero (Table 5). Thus, taking into account the concentrations of solutions of heavy metal salts, the exchange capacity of Mn minerals, the quantity of exchange cations passing into solutions, and the pH of equilibrium solutions, one may state that the mechanism responsible for sorption of Ni^{2+}, Zn^{2+}, and Cd^{2+} is equivalent irrespective of the concentrations of these solutions, while the mechanism of Co^{2+}, Cu^{2+},

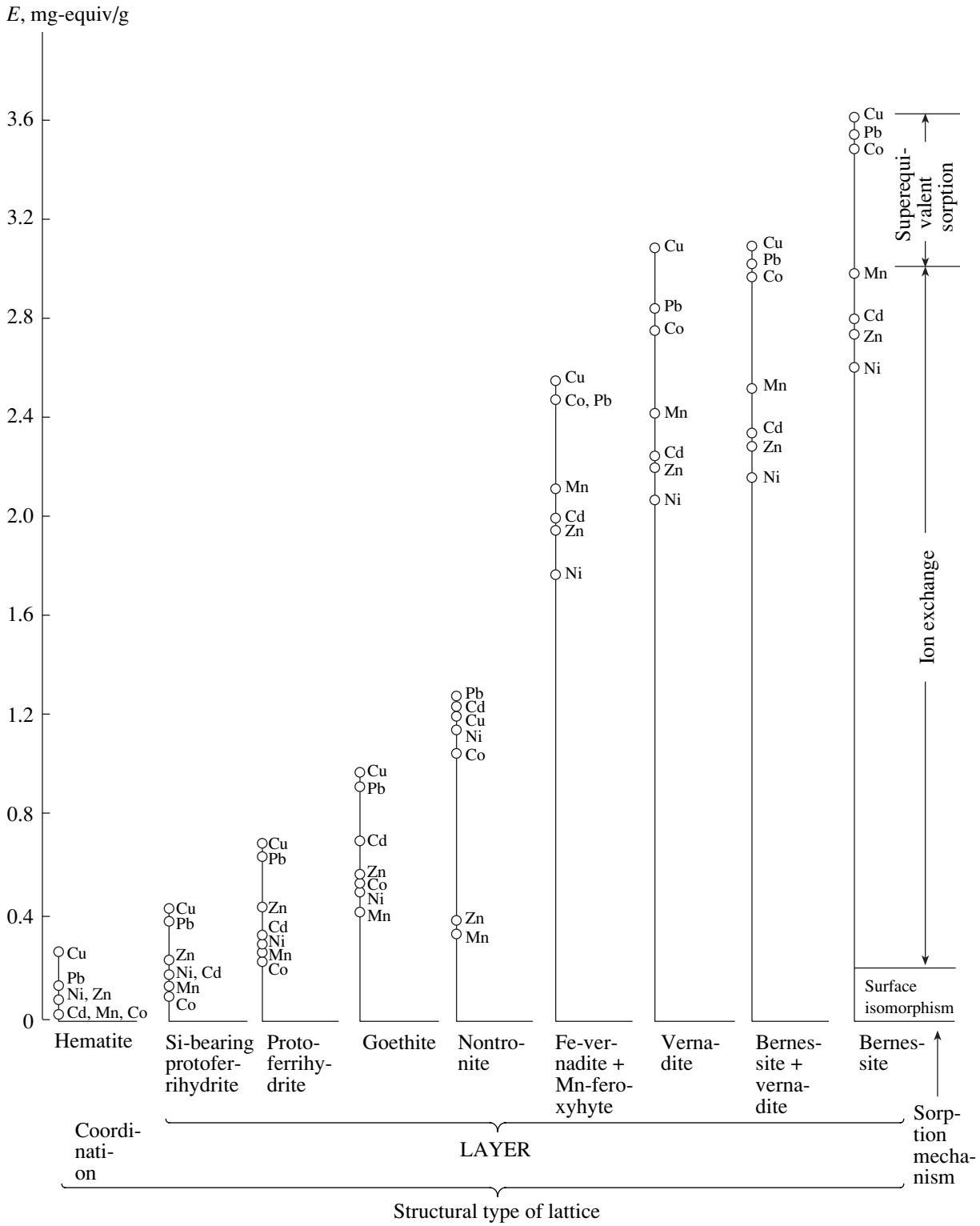

Fig. 3. Relationships between sorption and mineralogical characteristics of ferruginous and manganese deposits.

and Pb^{2+} sorption is superequivalent relative to the exchange cations of metals, Mn^{2+} included, in the case of their sorption from 1.0–0.01 N solutions and is equivalent in sorption from 0.001 N solutions. The equivalent exchange in sorption of Co^{2+} Cu^{2+}, and Pb^{2+} from diluted (0.001 N) solutions with the pH approaching the neutral value indicates the decreased role of protons H^+ in exchange reactions.

The role of Fe and its minerals in sorption of ore matter in Fe–Mn deposits was considered by Chelishchev et al. (1992), Novikov (1996), and Novikov and Skornyakova (1998). On the one hand, the experimental data on sorption of ions of heavy and rare metals by nodules and crusts of different chemical and mineral compositions demonstrated a low sorption activity of Fe minerals with respect to the metal cations. On the other hand, the data obtained allowed the suggestion that, in addition to isomorphic replacement of structural Mn(IV) in MnO_6 layers, Fe(III) also occupies other sites in Mn minerals, from where it is not displaced into solution by ions of heavy and rare metals, thereby reducing the exchange capacity of minerals.

This study confirmed the above assumptions. Let us compare the sorption of heavy metal cations in two groups of samples. The first group consists of samples 2192-3 and 1883-5, composed of Fe-free vernadite and Fe-vernadite + Mn-feroxyhyte, respectively. The latter minerals are close in Mn contents of 21.52 and 19.66 wt % and substantially differ (by more than an order of magnitude) in Fe contents of 1.45 and 16.15 wt %, respectively (Table 1). The exchange capacity of Fe-free vernadite with respect to heavy metal cations exceeds by 0.16–0.27 mg-equiv/g that of the Fe-vernadite + Mn-feroxyhyte assemblage. Hence, the occurrence of Fe in the sample reduces the absorptive properties of vernadite.

The second group is made up of separate layers of sample 2202-2A2, where both the mineral composition and the Mn and Fe contents change from the surface toward central parts (Table 1). The external (0–1 cm) layer of the sample, consisting of Fe-vernadite and Mn-feroxyhyte, is characterized by an exchange capacity ranging from 2.24 (Ni) to 3.35 (Cu) mg-equiv/g. In two underlying layers of this sample (1–4 cm), composed largely of Si-bearing protoferrihydrite, this parameter ranges from 0.31 to 0.80 mg-equiv/g (1–2 cm) and from 0.012 to 0.51 mg-equiv/g (2–4 cm). The higher exchange capacity of the second layer (1–2 cm) with respect to all heavy metal cations is explained by an admixture of vernadite (the Mn content is 6.15 wt %). The comparative analysis of the sorption activity of Mn and Fe minerals explains, in our opinion, the difference in contents of heavy metals in natural samples.

Thus, the high sorption activity of low-temperature hydrothermal and hydrogenic Mn minerals is largely determined by their crystallochemical properties, the content of quadrivalent Mn (MnO_2) in samples, and the selective sorption with respect to heavy metal cations.

The coefficients of mineral enrichment (K_{enrich}) as a ratio of absorptivity values of different minerals with respect to the given cations are also indicative of substantially higher sorption activity of Mn minerals than Fe minerals and nontronite of any genesis. The highest K_{enrich} values with respect to Cd are established for Mn minerals and nontronite relative to hematite: 66.6–92.6 and 41.3, respectively (Table 6). The absorptive capacity of nontronite with respect to all heavy metals is, in turn, higher than that of Fe minerals (K_{enrich} is 1.23–41.3). Mn^{2+} and Zn^{2+} are the only exception: K_{enrich} for these cations is <1 for the nontronite–goethite and nontronite–protoferrihydrite pairs. Goethite and protoferrihydrite likely reveal a higher selectivity relative to these cations in comparison with nontronite. Minimal K_{enrich} values are established with respect to either Cu (2.59–12.8 in 14 of 19 ratios) or Pb (2.64–6.74) (Table 6).

CONCLUSIONS

The obtained data on the sorption activity of oceanic low-temperature hydrothermal and hydrogenic deposits of different mineral and chemical compositions provide insights into some general relationships.

All examined minerals and their assemblages are able to exchange with metal cations in solutions, although the exchange degree is different for each class of minerals and is controlled by their structural, crystallochemical, and physicochemical properties, as well as by the chemical nature of absorbed metal cations. Thus, these natural compounds are natural ion exchangers.

The sorption activity of low-temperature minerals from Pacific hydrothermal fields increases in the following succession: hematite ⩽ Si-bearing protoferrihydrite < protoferrihydrite < goethite < nontronite ⩽ Fe-vernadite + Mn-feroxyhyte < Fe-free vernadite < bernessite + Fe-free vernadite < bernessite, i.e., increases from the mineral with a coordination type of lattice toward minerals with a layer structure.

By exchange capacity, the minerals are divided into four groups. The first group includes hematite, characterized by a very low capacity (up to 0.1 mg-equiv/g), in which the cation exchange is realized by surface isomorphic replacements (Novikov and Cherkashev, 2000). The second group consists of protoferrihydrite and goethite, whose exchange capacity varies from 0.23 to 0.98 mg-equiv/g. The third group is represented by nontronite, whose capacity ranges from 1.04 to 1.30 mg-equiv/g with respect to most of the examined cations and from 0.34 to 0.43 mg-equiv/g with respect to Mn^{2+} and Zn^{2+}. The mechanism of absorption of heavy metal cations by minerals of the second and third groups is equivalent. The fourth group is composed of Mn minerals, which reveal striking sorption properties irrespective of their genesis and are characterized by a high capacity relative to heavy metal cations (1.42–3.58 mg-equiv/g). The exchange capacity within this group increases distinctly from hydrogenic Fe-vernadite toward hydrothermal bernessite and Fe-free vernadite. The sorption of Ni^{2+}, Cd^{2+}, Zn^{2+}, and Mn^{2+} proceeds in line with the equivalent ion exchange mechanism (as in the case of minerals belonging to the second and third groups) at any concentration of metal salt solutions. The sorption of Co^{2+}, Pb^{2+}, and Cu^{2+} is superequivalent even taking into account Mn^{2+} in the exchange complex of minerals when these cations are

absorbed from concentrated solutions and equivalent when they are absorbed from diluted solutions.

As can be seen from Table 2, two series of the absorbed metal cations are distinguished. As concerns Fe–Mn minerals, these series are identical. The difference consists only in the combination of Co^{2+} with Pb^{2+} and Cu^{2+} into a common series in Mn minerals. The series for nontronite reveals a difference accounted for by its lower selectivity with respect to Mn^{2+} and Zn^{2+} relative to other heavy metal cations.

The study of products of ion-exchanging reactions carried out by electron microdiffraction did not establish new phases despite high contents of heavy metal cations, particularly Pd^{2+}, Cd^{2+}, and Cu^{2+}, in examined minerals, primarily, in Mn varieties.

The exchange complex of minerals distinct in chemical composition, lattice structure, and genesis consists of Na^+, K^+, Ca^{2+}, and Mg^{2+}, i.e., of the main cations of seawater. Mn minerals, irrespective of their genesis, include also Mn^{2+} as a main exchange component, which makes a substantial contribution to the exchange capacity of these minerals (up to 0.5 mg-equiv/g) and thus redistributes the shares of the other cations in the total capacity. The contribution of all the above cations to the exchange capacity of minerals amounts to 90–98%. Ni^{2+}, Cu^{2+}, and Zn^{2+} are involved in exchange reactions with participation of Mn minerals, although their contribution to the capacity of minerals is insignificant: 0.05–0.07 mg-equiv/g, or 2.0–3.5 wt % of their content in samples.

The differences in ion-exchanging properties of samples similar in genesis but different in chemical and mineral compositions are substantially greater than in the case of samples composed of minerals of the same class but belonging to different genetic groups. Thus, the crystallochemical and physicochemical properties of natural minerals are their most important characteristics for the process under consideration. The sorption activity of low-temperature hydrothermal fields is primarily determined by their mineral composition, while the role of the genetic factor is significantly lower.

ACKNOWLEDGMENTS

This work was supported by the Russian Academy of Sciences (the program of the Presidium of the Russian Academy of Sciences "Fundamental Problems of Oceanology") and the Russian Foundation for Basic Research, project nos. 03-05-64346, 03-05-65005, and 06-05-64614.

REFERENCES

1. S. I. Andreev, *Metallogeny of Ferromanganese Nodules in the Pacific Ocean* (Nedra, St. Petersburg, 1994) [in Russian].
2. M. J. Angove, B. B. Johnson, and J. D. Wells, "The Influence of Temperature on the Adsorption of Cadmium (II) and Cobalt (II) on Kaolinite," J. Colloid Interface Sci. **204**, 93–103 (1998).
3. E. S. Bazilevskaya, "Mobile Manganese Forms and Associated Elements in Ferromanganese Nodules and Sediments Derived by Acid Extraction," in *Ferromanganese Nodules in the Central Pacific Ocean* (Nauka, Moscow, 1986), pp. 238–250 [in Russian].
4. R. A. Binns, S. D. Scott, Yu. A. Bogdanov, et al., "Hydrothermal Oxide and Gold-Rich Sulfate Deposits of the Franklin Seamount, Western Woodlark Basin, Papua New Guinea," Econ. Geol. **88**, 2122–2153 (1993).
5. Yu. A. Bogdanov, E. G. Gurvich, O. Yu. Bogdanova, et al., "Low-Temperature Deposits of the Logachev Hydrothermal Field, the Mid-Atlantic Ridge," Geol. Rudn. Mestorozhd. **46** (4), 313–331 (2004) [Geol. Ore Deposits **46** (4), 269–285 (2004)].
6. Yu. A. Bogdanov and A. P. Lisitsyn, "Specific Composition of Hydrothermal Rocks. Causes of Hydrothermal Substance Differentiation," in *Geological Structure and Hydrothermal Deposits of the Juan de Fuca Ridge* (Nauka, Moscow, 1990), pp. 80–86 [in Russian].
7. Yu. A. Bogdanov, A. P. Lisitzyn, R. A. Binns, et al., "Low-Temperature Hydrothermal Deposits of the Franklin Seamount, Woodlark Basin, Papua New Guinea," Mar. Geol. **142**, 99–117 (1997).
8. O. Yu. Bogdanova and A. I. Gorshkov, "Petrography and Mineralogy of Ferromanganese Ores," in *Geology of the Tadjura Rift: Observations from Manned Submersibles* (Nauka, Moscow, 1987), pp. 194–200 [in Russian].
9. O. Yu. Bogdanova, A. I. Gorshkov, and G. A. Dubinina, "Origin of Ferric–Ferrous and Manganese Oxides," in *Geological Structure and Hydrothermal Deposits in the Juan de Fuca Ridge* (Nauka, Moscow, 1990), pp. 77–80 [in Russian].
10. D. W. Breck, *Zeolitic Molecular Sieves* (Wiley, New York, 1973; Mir, Moscow, 1976).
11. G. Yu. Butuzova, *Hydrothermal Sedimentary Mineralization in the Red Sea Rift Zone* (GEOS, Moscow, 1998) [in Russian].
12. N. F. Chelishchev, *Ion Exchange Properties of Minerals* (Nauka, Moscow, 1973) [in Russian].
13. N. F. Chelishchev, N. K. Gribanova, and G. V. Novikov, *Sorption Properties of Oceanic Ferromanganese Nodules and Crusts* (Nedra, Moscow, 1992) [in Russian].
14. N. F. Chelishchev, V. F. Volodin, and V. L. Kryukov, "Ion Exchange Properties of Natural Highly Siliceous Zeolites" (Nauka, Moscow, 1988) [in Russian].
15. D. Cronan, *Underwater Minerals* (Academic Press, 1980; Mir, Moscow, 1982).
16. W. A. Deer, R. A. Howie, and J. Zussman, *Rock-Forming Minerals* (Wiley, New York, 1962; Mir, Moscow, 1966).
17. A. I. Gorshkov, V. A. Drits, G. A. Dubinina, et al., "Crystall Chemistry, Origin, and Mineralogy of Fe- and Fe–Mn Deposits from the Hydrothermal Field of the Franklin Seamount," Litol. Polezn. Iskop. **27** (4), 3–14 (1992).
18. Yu. A. Kokotov, *Ions and Ion Exchange* (Khimiya, Moscow, 1980) [in Russian].
19. J. R. Lead, J. Hamilton-Taylor, W. Davison, and M. Harper, "Trace Metal Sorption by Natural Particles and Coarse Colloids," Geochim. Cosmochim. Acta **63** (11/12), 1661–1670 (1999).

20. A. P. Lisitsyn, R. A. Binns, Yu. A. Bogdanov, et al., "Recent Hydrothermal Activity of the Franklin Seamount in the Western Woodlark Sea (Papua New Guinea)," Izv. Akad. Nauk SSSR, Ser. Geol., No. 8, 125–140 (1991).

21. G. V. Novikov, "Oceanic Ferromanganese Nodules—Metal Ion Sorbents: Chemical–Mineralogical Aspects," Zap. Vseross. Mineral. O–va **125** (3), 38–51 (1996).

22. G. V. Novikov, *Methods of Estimation of Sorption Properties of Ferromanganese Deposits in the World Ocean* (Granitsa, Moscow, 2005) [in Russian].

23. G. V. Novikov, S. I. Andreev, and L. I. Anikeeva, "Sorption Activity of Ferromanganese Nodules in Ocean," in *Oceanic Lithosphere: Composition, Structure, Evolution, Forecast, and Estimation of Mineral Resources* (VNIIOkeangeologiya, St. Petersburg, 1995), pp. 291–304 [in Russian].

24. G. V. Novikov and G. A. Cherkashev, "Ion-Exchange Reactions on Low-Temperature Oceanic Hydrothermal Rocks," Geochem. Intern. **38** (Suppl. 2), 194–205 (2000).

25. G. V. Novikov and N. S. Skornyakova, "Sorption Properties of Oceanic Ferromanganese Nodules and Crusts," Geokhimiya **36** (5), 505–517 (1998) [Geochem. Intern. **36** (5), 444–454 (1998)].

26. G. V. Novikov and S. V. Yashina, "Geochemistry, Mineralogy, and Sorption Properties of Cobalt–Manganese Crusts in the Pacific Ocean (Magellan Seamounts)," in *Cobalt-Bearing Ferromanganese Crusts of the Pacific Ocean* (VNIIOkeangeologiya, St. Petersburg, 1993), pp. 72–81 [in Russian].

27. A. I. Ponomarev, *Methods of Chemical Analysis of Silicate and Carbonate Rocks* (Izd. Akad. Nauk SSSR, Moscow, 1963) [in Russian].

28. H. Schneiderhöhn, "Genetische Lagerstattengliederung auf geotektonischer Grundlage," Neues Jahrb. Monatsh., No. 2, 47–63; No. 3, 65–89 (1952).

29. N. M. Strakhov, L. M. Shterenberg, and V. V. Kalinenko, "Geochemistry of Sedimentary Manganese-Ore Process" (Izd. Akad. Nauk SSSR, Moscow, 1968) [in Russian].

30. Y. Takahashi, Y. Minai, S. Ambe, et al., "Comparison of Adsorption Behavior of Multiple Inorganic Ions on Kaolinite and Silica in the Presence of Humic Acid Using the Multitracer Technique," Geochim. Cosmochim. Acta **63**, 815–836 (1999).

31. Yu. I. Tarasevich and F. D. Ovcharenko, *Adsorption on Clay Minerals* (Naukova Dumka, Kiev, 1975) [in Russian].

32. I. I. Volkov, "Ferromanganese Nodules," in *Geochemistry of Bottom Sediments* (Nauka, Moscow, 1979), Vol. 2, pp. 441–467 [in Russian].

33. E. D. Zaitseva, "Exchange Volume and Exchange Cations in Sediments of the Pacific Ocean," in *Chemistry of the Pacific Ocean* (Nauka, Moscow, 1966), pp. 271–88 [in Russian].

34. F. V. Zuzuk and V. L. Kryukov, "Nickel Sorption by the Minerals from Zones of Weathering," Geokhimiya **25** (6), 855–861 (1987).